Comparison of ^{18}O + ^{12}C at 16.7 MeV/nucleon reaction with the AMD+GEMINI++ model

Lucia Baldesi[1,2,*], *Sandro* Barlini[1,2], *Andrea* Stefanini[1,2], *Alberto* Camaiani[1,2], *Silvia* Piantelli[2], *Giovanni* Casini[2], *Caterina* Ciampi[3], *Marco* Cinausero[4], *Magda* Cicerchia[5], *Daniele* Dell'Aquila[6,7], *Lorenzo* Domenichetti[8], *Daniela* Fabris[9], *Catalin* Frosin[1,2], *Andrea* Gozzelino[4], *Ivano* Lombardo[10,11], *Tommaso* Marchi[4], *Sandra* Moretto[5,9], *Alberto* Mengarelli[12], *Alessandro* Olmi[2], *Gabriele* Pasquali[1,2], *Luca* Scomparin[13], *Simone* Valdré[2], and *Eleonora* Vanzan[5,9]

[1]Dipartimento di Fisica, Università di Firenze - Sesto Fiorentino, Italy
[2]INFN, Sezione di Firenze - Sesto Fiorentino, Italy
[3]Grand Accélérateur National d'Ions Lourds (GANIL), CEA/DRFCNRS/IN2P3, Boulevard Henri Becquerel - Caen, France
[4]INFN Laboratori Nazionali di Legnaro - Legnaro, Italy
[5]Dipartimento di Fisica, Università di Padova - Padova, Italy
[6]Dipartimento di Fisica Ettore Pancini, Università di Napoli Federico II - Napoli, Italy
[7]INFN Sezione di Napoli - Napoli, Italy
[8]Institut Laue-Langevin, 71 Av, des Martyrs - Grenoble , France
[9]INFN Sezione di Padova - Padova, Italy
[10]INFN Sezione di Catania - Catania, Italy
[11]Dipartimento di Fisica e Astronomia, Università di Catania - Catania, Italy
[12]INFN Sezione di Bologna - Bologna, Italy
[13]Karlsruher Institut für Technologie, Kaiserstraße 12 - Karlsruhe, Deutschland

Abstract. This study examines the performance of the antisymmetrized molecular dynamics (AMD) transport model in simulating the low-energy nuclear reactions ^{18}O + ^{12}C at 16.7 MeV/nucleon. Experimental data, collected using the GARFIELD+RCo detector at the Laboratori Nazionali di Legnaro, were compared with the AMD model coupled with the GEMINI++ decay code. The results show that the model accurately predicts the behaviour of fragments with $Z \geq 10$, although discrepancies were observed in the production of fragments with $4 < Z < 10$.

1 Introduction

Nuclear reactions at energies above 10 MeV/nucleon are characterized by various mechanisms. In fact, beyond complete fusion, which is the dominant mechanism at lower energies, other processes such as incomplete fusion and direct reactions become significant. For the ^{18}O + ^{12}C reaction at 16.7 MeV/nucleon the systematics from [1] estimates that the fusion cross section accounts for approximately 17% of the total, shared between complete (11%) and incomplete (6%) fusion. A similar estimation can be found using the systematics in [2], which suggests a 15.5% contribution from complete fusion. As a result, a substantial fraction of the reaction cross section remains unexplained by statistical models, necessitating the use of an alternative approach. In particular, we employed the antisymmetrized molecular dynamics (AMD) model [3], coupled with GEMINI++ [4] as afterburner. The AMD model is commonly used to simulate reactions at higher energies involving both intermediate-mass systems [5–8] and light systems [9–12]. This work, as further detailed in [13], represents the first application of the AMD model on a light system at such a low energy.

2 Experimental apparatus and theoretical model

The experiment took place at the Laboratori Nazionali di Legnaro (LNL, Italy). A ^{18}O beam at 300 MeV was delivered by the ALPI Linac on a ^{12}C target. The reaction products were detected using the GARFIELD+RCo setup [14]. This apparatus provides a geometric efficiency of roughly 80% of the total solid angle and high granularity, featuring nearly 300 ΔE-E telescopes. The GARFIELD detector is dedicated to the detection of Light Charged Particles (LCPs) and Intermediate Mass Fragments (IMFs). The RCo is designed to detect also heavier fragments, such as evaporation residues.

As previously mentioned, the transport model AMD [3] was employed. Approximately 130000 events were generated following a triangular probability distribution of the impact parameter up to the grazing value (8 fm). The excited fragments produced at the end of the dynamic phase (calculated up to 500 fm/c) was used as input for the

*e-mail: lucia.baldesi@fi.infn.it

statistical code GEMINI++. In order to increase the statistics, 1000 secondary events were generated for each primary one. Before comparing with experimental data, the simulated events were filtered through a software replica of the apparatus, which takes into account the angular coverage, the energy threshold and the energy resolution of each detector.

3 Experimental results and analysis

In the analysis, we impose the conditions $5 < Z_{tot} < 15$ and $0.3 < p_{tot}/p_{beam} < 1.1$ and we select only those events with a charged particle multiplicity greater than one. We will focus on fragments with $Z > 2$, which are mainly produced at forward angles. Therefore, we select fragments detected in the RCo allowing for better angular, energy and mass resolution. In Fig. 1, the comparison of the experimental and simulated velocity distributions of some of these fragments is shown. For fragments with Z = 3, 4 and

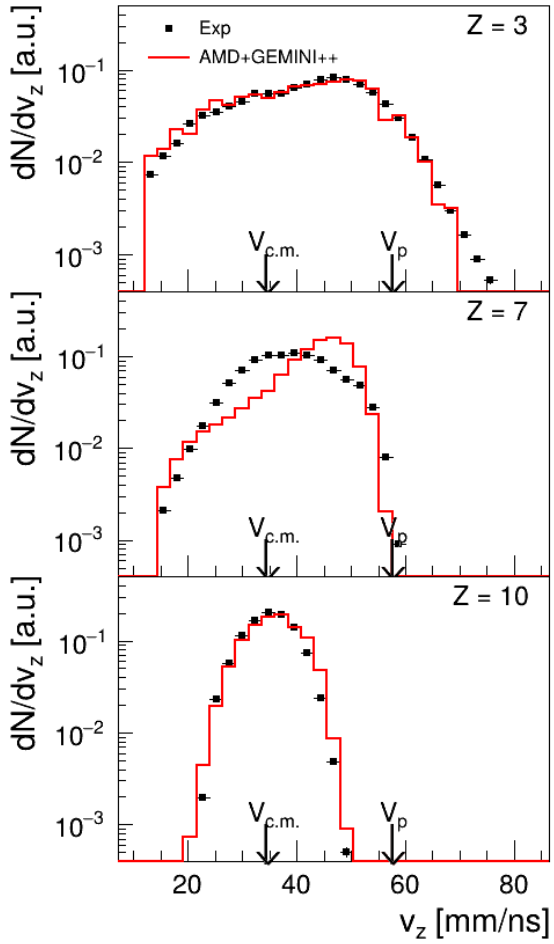

Figure 1: Velocity v_z distributions normalized to the area for fragments with Z = 3, 7, 10. Black markers: experimental distributions. Red lines: AMD+GEMINI++ distributions.

$Z \geq 10$, the AMD+GEMINI++ simulations show good agreement with the experimental data. The spectra of fragments with $Z \geq 10$ are particularly noteworthy, as their peak is close $v_{c.m.}$. This suggests that these heavy fragments are likely produced through complete or incomplete fusion processes. Given their origin, which is also confirmed by the model [13], it is possible to perform a quantitative comparison between the experimental data and the model predictions to distinguish between the contributions of complete and incomplete fusion using a two Gaussian fit of the velocity distributions, as proposed in [15]. In Fig. 2 the results of the Gaussian fit on the experimental (left panel) and filtered model (right panel) spectra for fragments with Z = 10 are shown. Similar results were obtained also for Z = 11 and 12. In the fit procedure, we fixed the mean and the width of the Gaussian which reproduces the complete fusion (green line) at the values suggested by the GEMINI++ code, while the parameters of the incomplete fusion Gaussian (blue line) were left free, with the only constraint for the mean to be located at $v > v_{c.m.}$. The results of this procedure confirm that ions with $Z \geq 10$ are mainly produced in central events, basically associated to fusion-like events. Moreover, the Gaussian fits

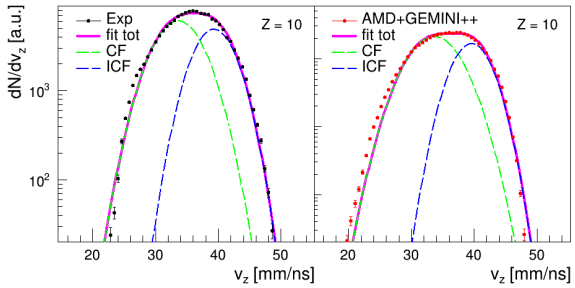

Figure 2: Velocity v_z distributions of Z = 10 for experimental (black, left panels) and AMD+GEMINI++ (red, right panels) data. The magenta solid line is the result of the two Gaussian fit, while the green (blue) dashed line represents the complete (incomplete) fusion component.

allow to deduce quantitatively the fractions of complete and incomplete fusion, as shown in Table 1 considering also their statistical and systematic errors. The experimental percentages are rather well reproduced by the filtered AMD+GEMINI++ simulation. Using the 4π simulation, we can also evaluate the impact of the apparatus filter: it results to be negligible for Z = 12, while it is sizable for Z = 10 and Z = 11 perhaps due to a larger effect of the modest coverage of the RCo.

For fragments with $5 < Z < 9$, the model predictions deviate from the experimental data, showing a preference for less dissipative events over fusion-like ones (Fig. 1). This tendency of the AMD model, already pointed out in [9], can be further explored by analysing the AMD+GEMINI++ velocity spectra as a function of the impact parameter b, as shown in Fig. 3. Fragments with Z = 6, 7, 8 produced in central collisions (b = 0 - 2) are emitted in phase-space regions that are associated with more peripheral reactions (b = 6 - 8), perhaps indi-

		exp (%)	**filtered simul** (%)	**4π simul** (%)
Z=10	**CF**	58.5±0.5±0.7	62.6±0.3±1.1	53.1±0.1±1.3
	ICF	40.9±0.6±0.8	36.7±0.3±1.2	45.8±0.1±1.5
Z=11	**CF**	61 ±1 ±6	64.9 ±0.4 ±4	59.9 ±0.1 ±4
	ICF	34 ±1 ±5	31.8 ±0.4 ±2	36.9 ±0.1 ±2
Z=12	**CF**	69 ±3 ±13	75 ±1 ±13	74.9 ±0.3 ±6
	ICF	22 ±2 ±7	18.0 ±0.7 ±6	20.8 ±0.2 ±3

Table 1: Percentages of complete and incomplete fusion with respect to the total as deduced from the two Gaussian fit on experimental, filtered and 4π model distributions. Statistical an systematic errors are listed.

cating too low dissipation predicted by the model. This effect could be related to the NN cross section value adopted by the model and/or to the inclusion of clustering interactions, which could unfavour on average the one-body dissipation. In this analysis, the AMD code was run with the standard parameters from [9], but future studies should focus on optimizing the AMD parameters to better reproduce this system. On the other hand, we could also investigate the de-excitation process, which in this case is simulated using the statistical code GEMINI++. In future studies we could explore the use of a multifragmentation model, such as SMM [16], which might result in a different momentum distribution compared to GEMINI++.

4 Conclusions

In this work, we have presented a comparison between experimental data and the AMD simulation for the ^{18}O+^{12}C reaction at 16.7 MeV/nucleon. To our knowledge, this is the first time that the AMD transport code has been tested for a light system at such low bombarding energy. The overall agreement between the experimental data and the AMD+GEMINI++ model is good for fragments with Z $\geq$ 10, which are expected to result from complete or incomplete fusion processes. In fact, the AMD+GEMINI++ model accurately reproduces their multiplicity, velocity spectra, and the percentages of complete and incomplete fusion events. However, the model tends to underpredict highly dissipative collisions in the most central impacts. This is evident from the underproduction of Z = 6, 7, 8 ions with characteristics of evaporation residues; instead, these fragments are mostly produced with velocity too close to the entrance channel. Future work will focus on both tuning the AMD parameters and exploring alternative de-excitation models to determine whether a better reproduction of our experimental data can be achieved.

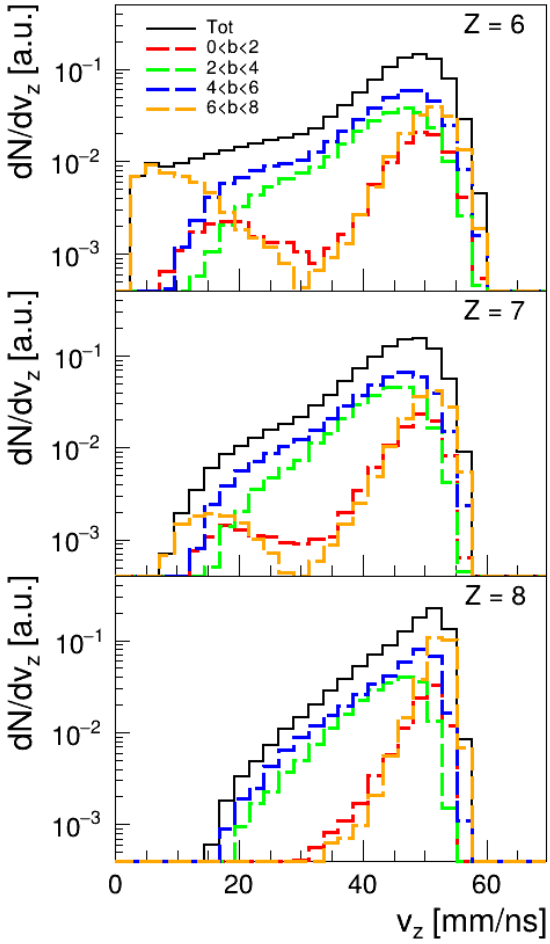

Figure 3: Model data in 4π: velocity v$_z$ distributions for secondary fragments with Z = 6, 7, 8. Black lines: total spectra. Colored lines: different selection of the impact parameter *b*.

References

[1] P. Eudes, Comprehensive analysis of fusion data well above the barrier. Phys. Rev. C **90**, 034609 (2014). https://doi.org/10.1103/PhysRevC.90.034609;

[2] D. Dell'Aquila, Modeling heavy-ion fusion cross section data via a novel artificial intelligence approach. J. Phys. G: Nucl. **50**, 015101 (2023). https://doi.org/10.1088/1361-6471/ac9ad1

[3] A. Ono, Antisymmetrized Version of Molecular Dynamics with Two-Nucleon Collisions and Its Application to Heavy Ion Reactions. Prog. Theor. Phys. **87**, 1185 (1992). https://doi.org/10.1143/ptp/87.5.1185

[4] R. J. Charity, Systematic description of evaporation spectra for light and heavy compound nuclei. Phys. Rev. C **87**, 014610 (2010). https://doi.org/10.1103/PhysRevC.82.014610

[5] S. Piantelli, Comparison between calculations with the AMD code and experimental data for peripheral collisions of ^{93}Nb+^{93}Nb,^{116}Sn at 38 MeV/nucleon. Phys. Rev. C **99**, 064616 (2019). https://doi.org/10.1103/PhysRevC.99.064616

[6] S. Piantelli, Dynamical fission of the quasiprojectile and isospin equilibration for the system ^{80}Kr+^{48}Ca at 35 MeV/nucleon. Phys. Rev. C **101**, 034613 (2020). https://doi.org/10.1103/PhysRevC.101.034613

[7] S. Piantelli, Isospin transport phenomena for the systems ^{80}Kr+^{40,48}Ca at 35 MeV/nucleon. Phys. Rev. C **103**, 014603 (2021). https://doi.org/10.1103/PhysRevC.103.014603

[8] A. Camaiani, Isospin diffusion measurement from the direct detection of a quasiprojectile remnant. Phys. Rev. C **103**, 014605 (2021). https://doi.org/10.1103/PhysRevC.103.014605

[9] C. Frosin, Examination of cluster production in excited light systems at Fermi energies from new experimental data and comparison with transport model calculations. Phys. Rev. C **107**, 044614 (2023). https://doi.org/10.1103/PhysRevC.107.044614

[10] G. Tian, Nuclear stopping and light charged particle emission in ^{12}C + ^{12}C at 95 MeV/nucleon. Phys. Rev. C **95**, 044613 (2017). https://doi.org/10.1103/PhysRevC.95.044613

[11] G. Tian, Cluster correlation and fragment emission in ^{12}C + ^{12}C at 95 MeV/nucleon . Phys. Rev. C **97**, 034610 (2018). https://doi.org/10.1103/PhysRevC.97.034610

[12] R. Han, Effects of cluster correlations on fragment emission in ^{12}C + ^{12}C at 50 MeV/nucleon. Phys. Rev. C **102**, 064617 (2020). https://doi.org/10.1103/PhysRevC.102.064617

[13] L. Baldesi, Performance of the antisymmetrized molecular dynamics transport model for low energy reactions: Comparison with experimental results for ^{18}O + ^{12}C at 16.7 MeV/nucleon. Phys. Rev. C **109**, 064618 (2024). https://doi.org/10.1103/PhysRevC.109.064618

[14] M. Bruno, GARFIELD + RCo digital upgrade: A modern set-up for mass and charge identification of heavy-ion reaction products. Eur. Phys. J. A **49**, 128 (2013). https://doi.org/10.1140/epja/i2013-13128-2

[15] S. Pirrone, Fusion and competing processes in the ^{32}S+^{12}C reaction at E(^{32}S)=19.5 MeV/nucleon. Phys. Rev. C **64**, 024610 (2001). https://doi.org/10.1103/PhysRevC.64.024610;

[16] J.P. Bondorf, Statistical multifragmentation of nuclei. , Phys. Rep. **257**, 133 (1995). https://doi.org/10.1016/0370-1573(94)00097-M;